

Supplementary Materials for  
**Suppression of marine heatwave activity by tropical cyclone–induced upper  
ocean cooling**

Iam-Fei Pun *et al.*

Corresponding author: Iam-Fei Pun, [ipun@ncu.edu.tw](mailto:ipun@ncu.edu.tw)

*Sci. Adv.* **11**, eadw8070 (2025)  
DOI: 10.1126/sciadv.adw8070

**This PDF file includes:**

Figs. S1 to S12  
Tables S1 to S3

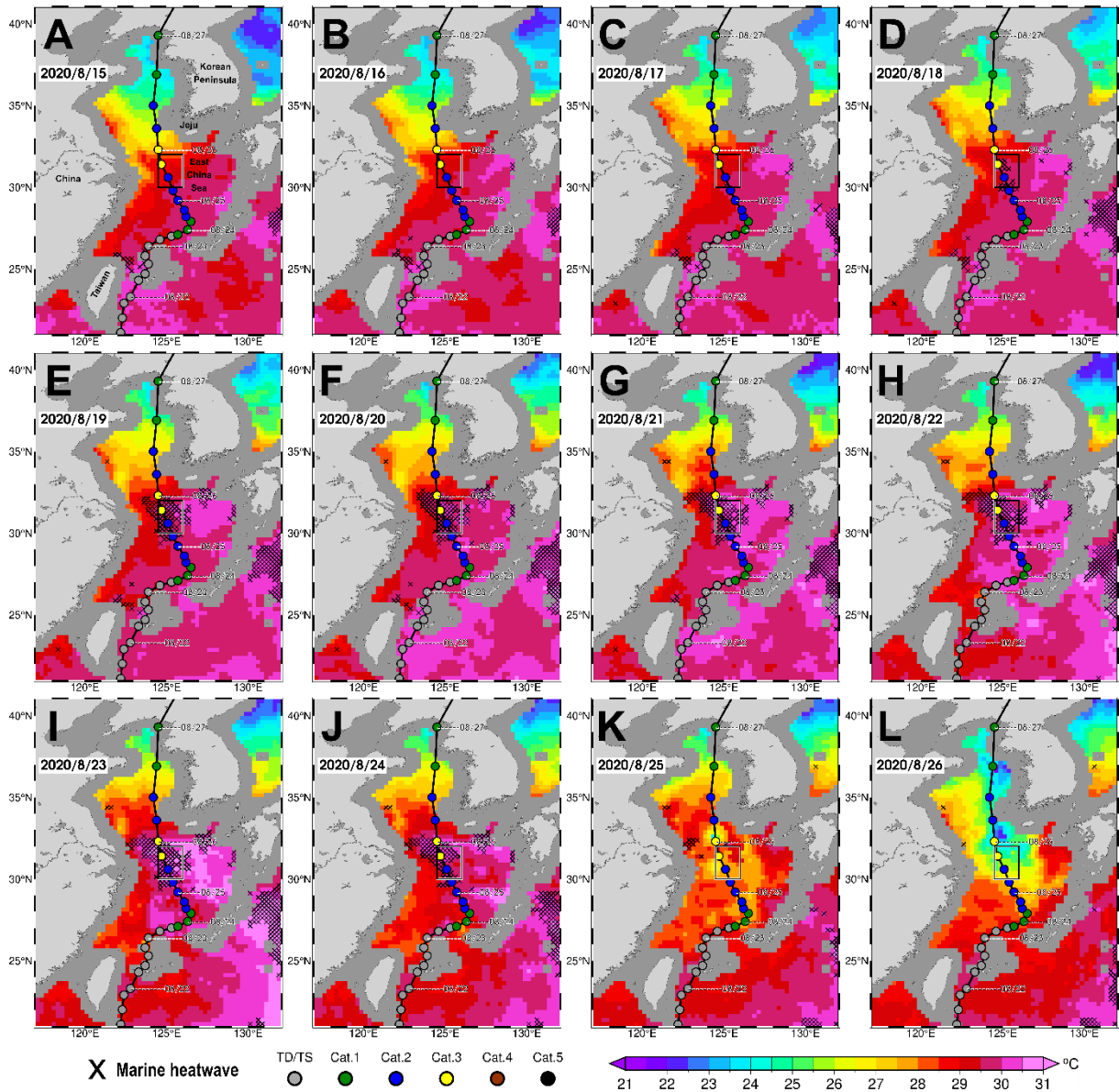


**Fig. S1.** Daily OISST maps for Tropical Cyclone Bavi. (A)-(L) SST from 15 August 2020 to 26 August 2020, covering the passage of Tropical Cyclone Bavi in the ECS. Note that the daily SST maps are synchronized to 1200 UTC. The 6-hourly TC track is shown with labels at each 0000 UTC. Cross marks represent the occurrence of marine heatwaves. Rectangle boxes indicate the averaged area for the SST evolution analysis in fig. S2. Geographic references are indicated in (A).

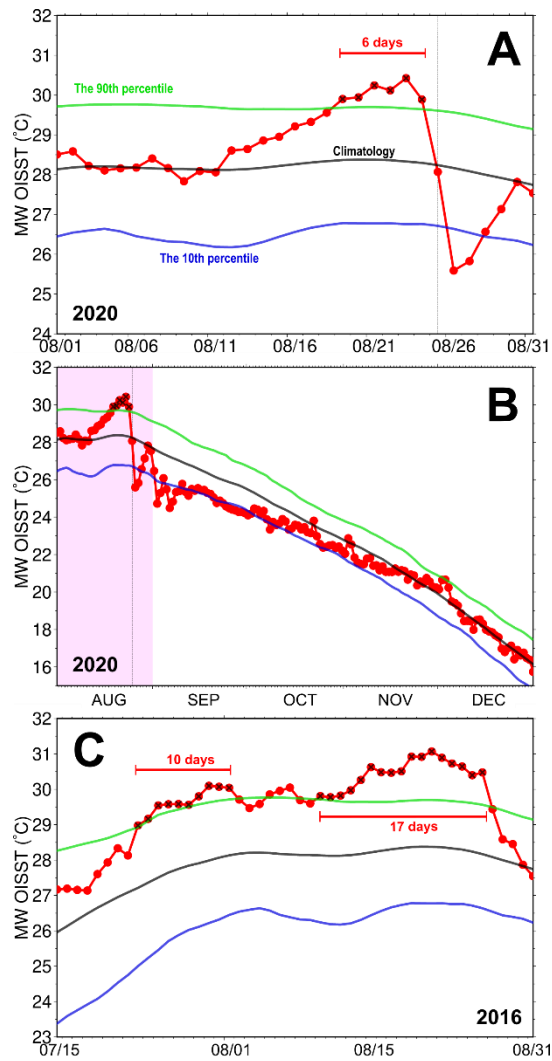


**Fig. S2. Area averaged daily SST time series analysis for Tropical Cyclone Bavi.** The area for average is indicated by the black rectangle box shown in fig. S1. Black curves show the daily climatology calculated from 1998 to 2023 from the OISST dataset, while the green and blue curves indicate the 90th and 10th percentiles. The days that classified as a MHW are marked by the cross marks. **(A)** The time series for August 2020. **(B)** Same as **(A)**, but for an extended period from August to December 2020. The pink shading indicates the period shown in **(A)**. Note that the MHW occurred prior to Tropical Cyclone Bavi. The vertical dashed lines represent the impact of the TC. **(C)** Same as **(A)**, but from 15 July to 31 August 2016, providing a comparison for the situation without TC influence. The duration of MHWs is indicated in **(A)** and **(C)**.

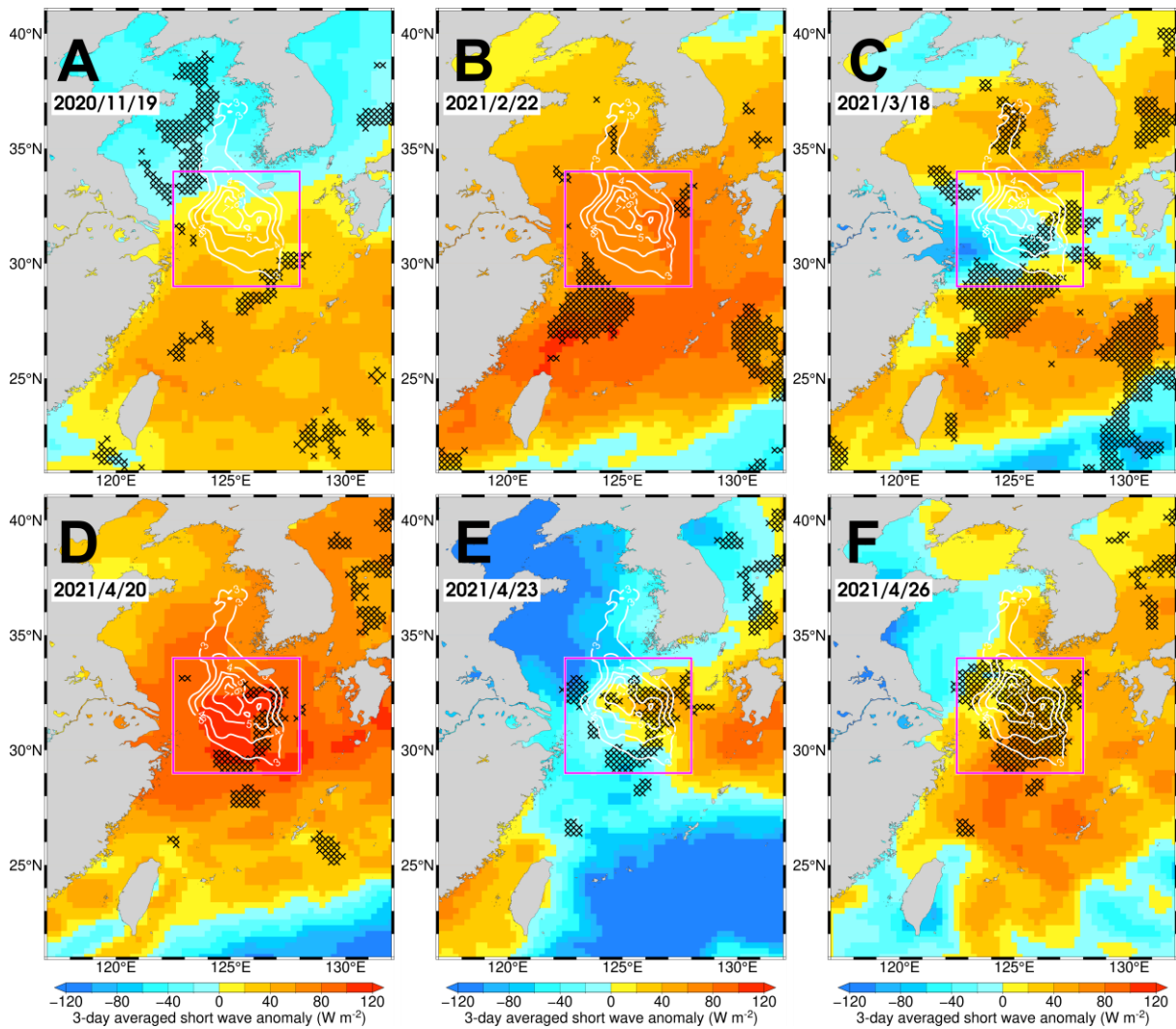


**Fig. S3. Surface net shortwave radiation anomalies for four MHW episodes following Bavi's passage.** (A) November 2020 episode. (B) February 2021 episode. (C) March 2021 episode. (D)-(F) April 2021 episode. The anomalies are 3-day averages, ending on the date indicated in each plot. Contours show the SST cooling induced by Tropical Cyclone Bavi at 1°C intervals, while black crosses denote the locations of MHWs, and the magenta box indicates the averaging area used for the ACI analysis shown in fig. S5.

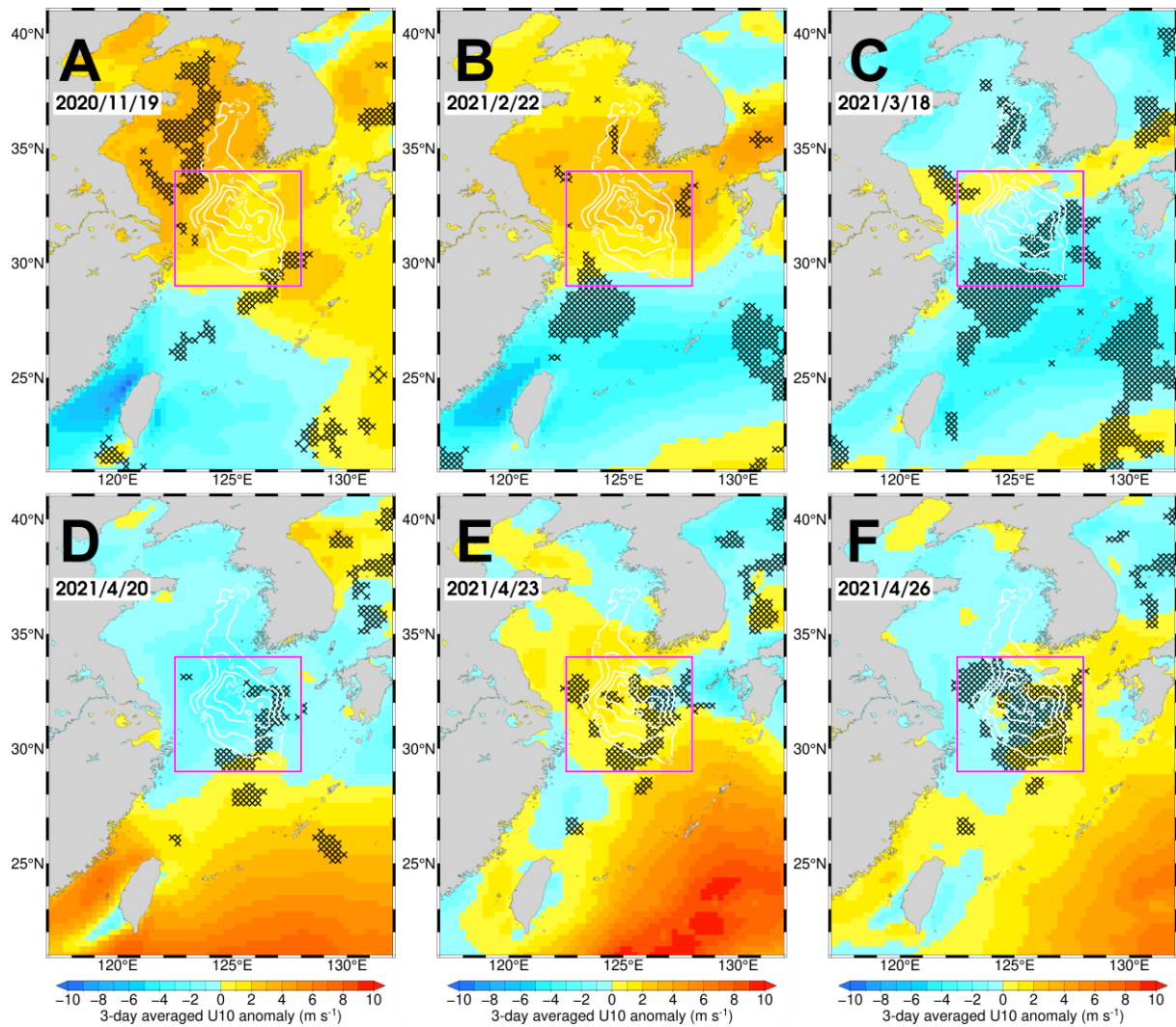


**Fig. S4. 10m wind speed anomalies for four MHW episodes following Bavi's passage. (A)** November 2020 episode. **(B)** February 2021 episode. **(C)** March 2021 episode. **(D)-(F)** April 2021 episode. The anomalies are 3-day averages, ending on the date indicated in each plot. Contours show the SST cooling induced by Tropical Cyclone Bavi at 1°C intervals, while black crosses denote the locations of MHWs, and the magenta box indicates the averaging area used for the ACI analysis shown in fig. S5.

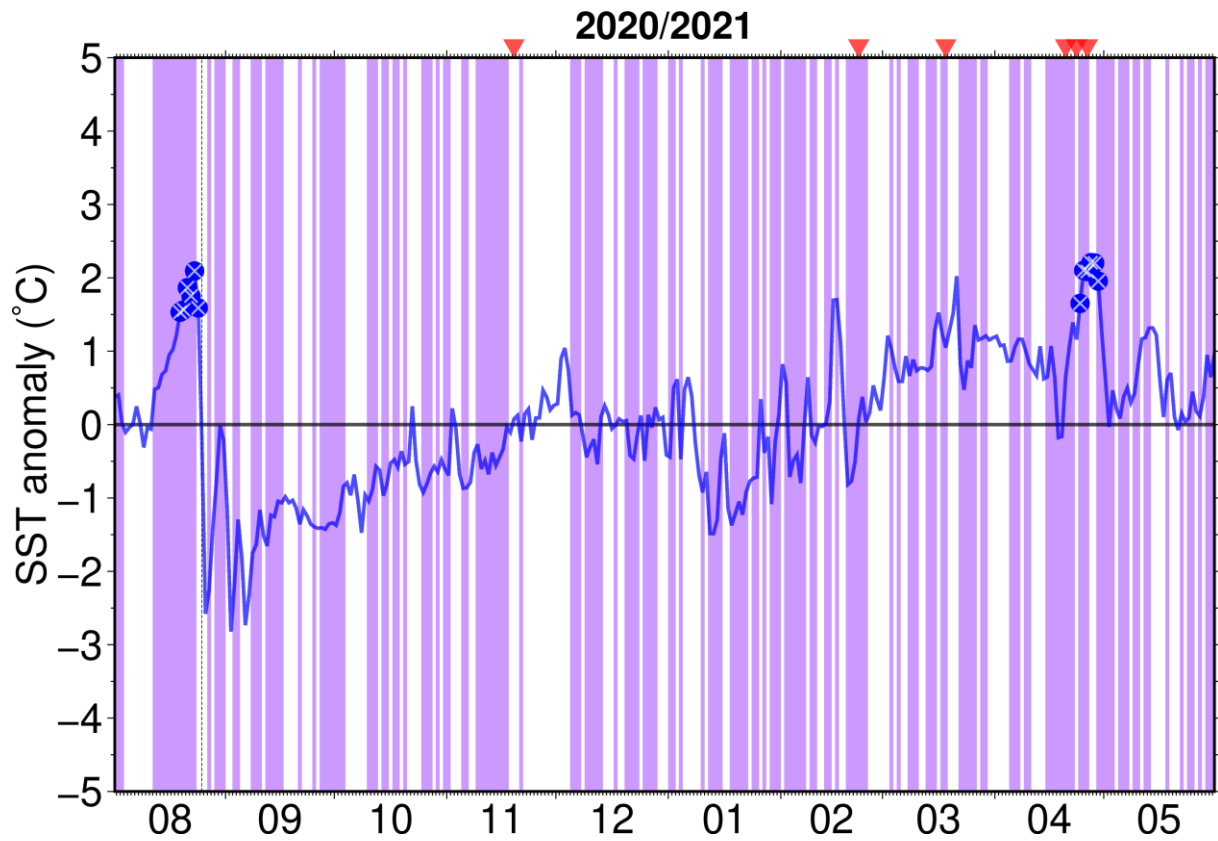


**Fig. S5. SST anomalies with ACI following Tropical Cyclone Bavi.** Averaged SST anomalies (relative to the 26-year baseline) from August 2020 to May 2021 over the SST cooling area induced by Bavi. Purple shading indicates periods with positive ACI values, averaged over the region outlined in figs. S3 and S4. Inverted triangles mark the four MHW episodes, while solid circles with crosses represent the days identified as MHWs. Notably, two MHW events (i.e., in August 2020 and April 2021) were generally associated with favorable atmospheric conditions, as indicated by the positive ACI.

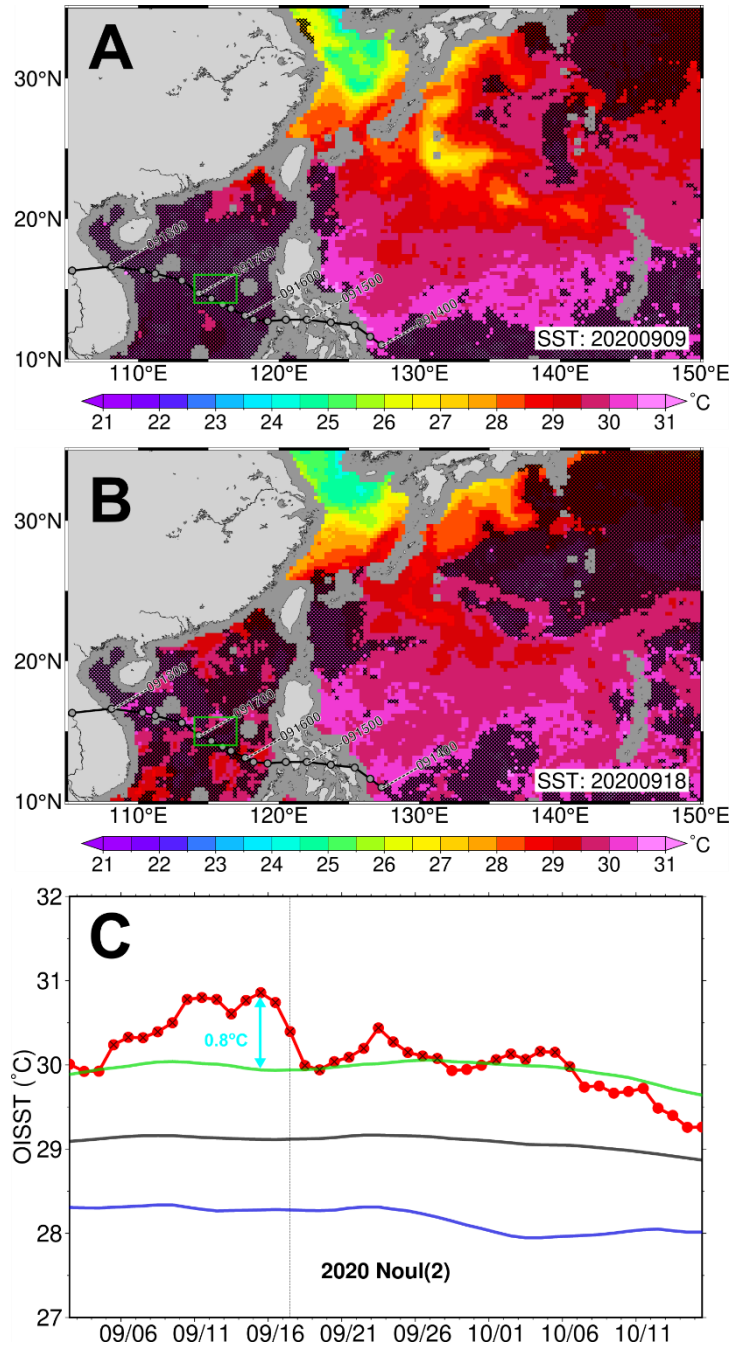


**Fig. S6. A TC-MHW case associated with Tropical Cyclone Noul (2020).** (A) SST map on 9 September 2020, showing conditions before the TC. (B) Same as (A), but for 18 September 2020 for conditions after the TC. Cross marks indicate the presence of MHW, and Noul's 6-hourly track is overlaid. (C) Time series of daily SST values averaged over the green box shown in (A) and (B). The black curve represents the climatological daily mean, while the green and blue curves indicate the 90th and 10th percentiles, respectively. The vertical dashed line represents the arrival of the TC, and SST cooling of 0.8°C induced by Noul is highlighted.

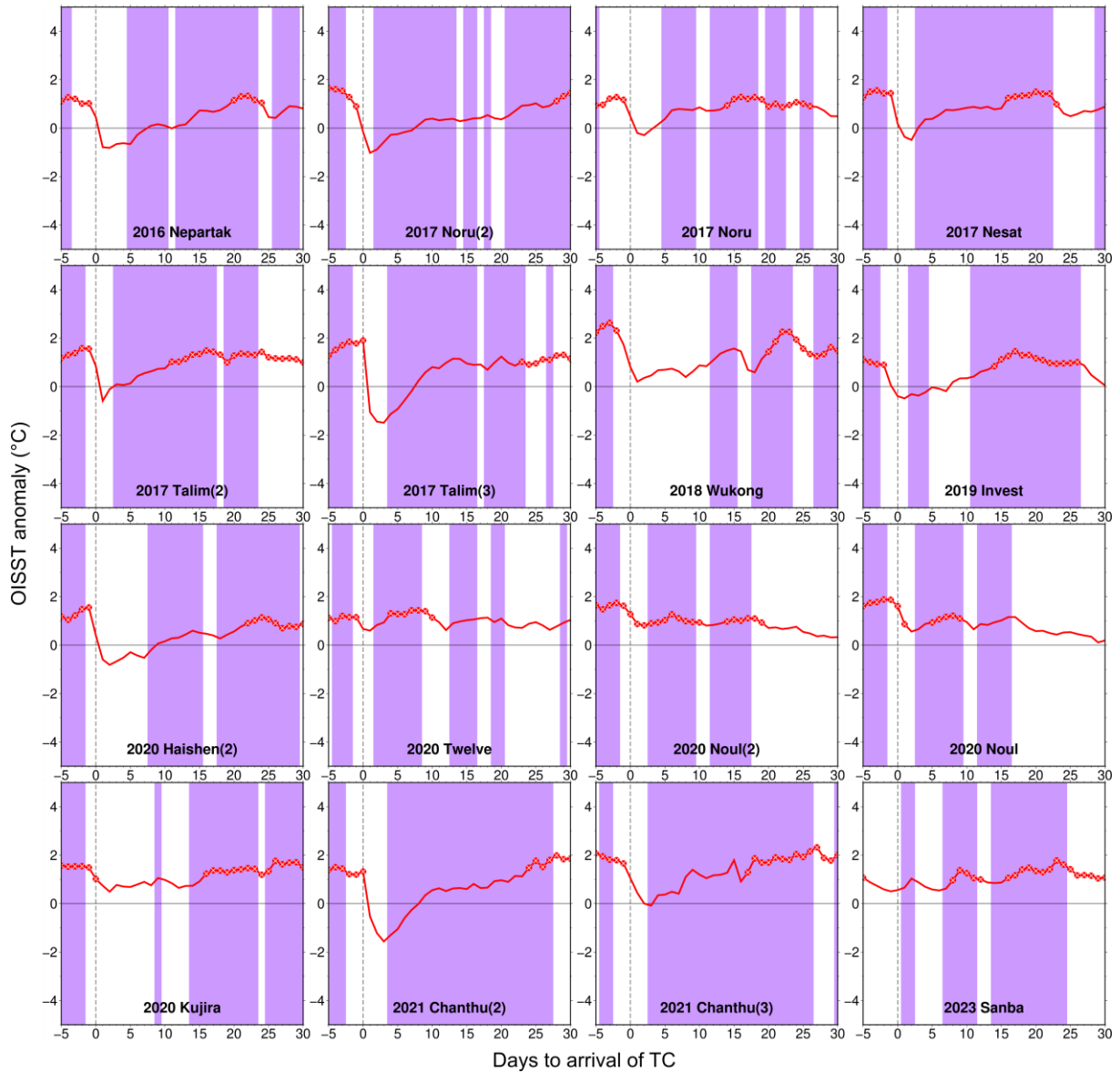


**Fig. S7. Sixteen TC-MHW cases with MHW recurrence within 30 days after TC passage and with a long pre-TC MHW duration ( $\geq 10$  days).** In each plot, the red curve represents SST anomalies relative to the 26-year daily climatological baseline. Solid circles with crosses mark the days identified as MHWs. The vertical dashed line indicates the impact of the TC. Purple shading denotes periods with positive ACI values, representing favorable atmospheric conditions for MHW development.

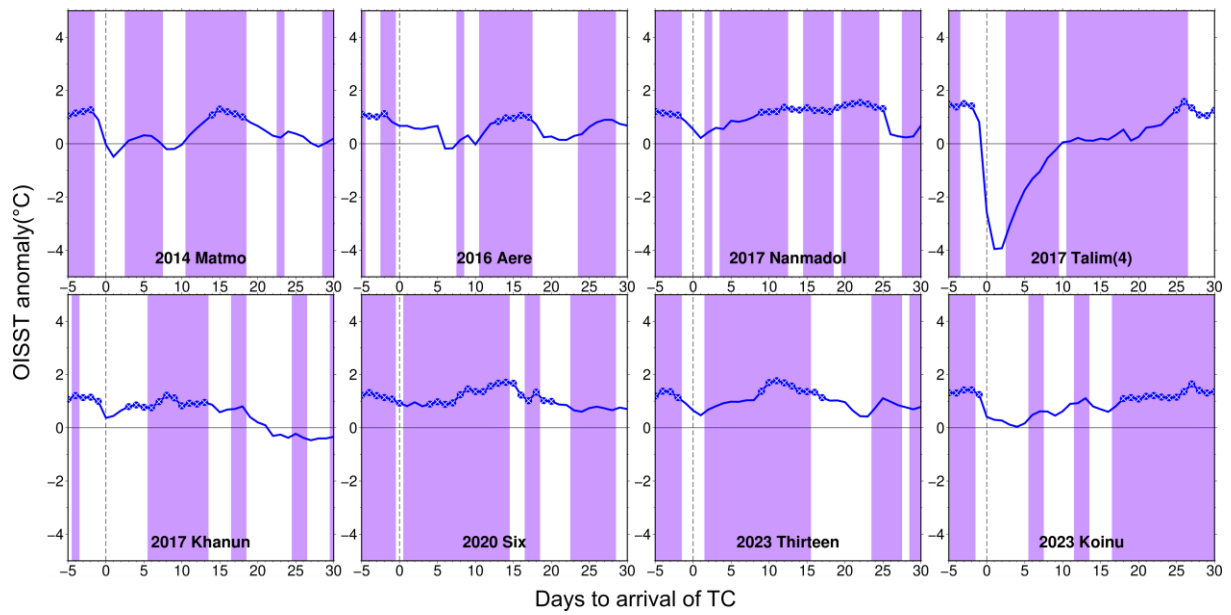


**Fig. S8. Eight TC-MHW cases with MHW recurrence within 30 days after TC passage but with a short pre-TC MHW duration (<10 days).** In each plot, the blue curve represents SST anomalies relative to the 26-year daily climatological baseline. Solid circles with crosses mark the days identified as MHWs. The vertical dashed line indicates the impact of the TC. Purple shading denotes periods with positive ACI values, representing favorable atmospheric conditions for MHW development.

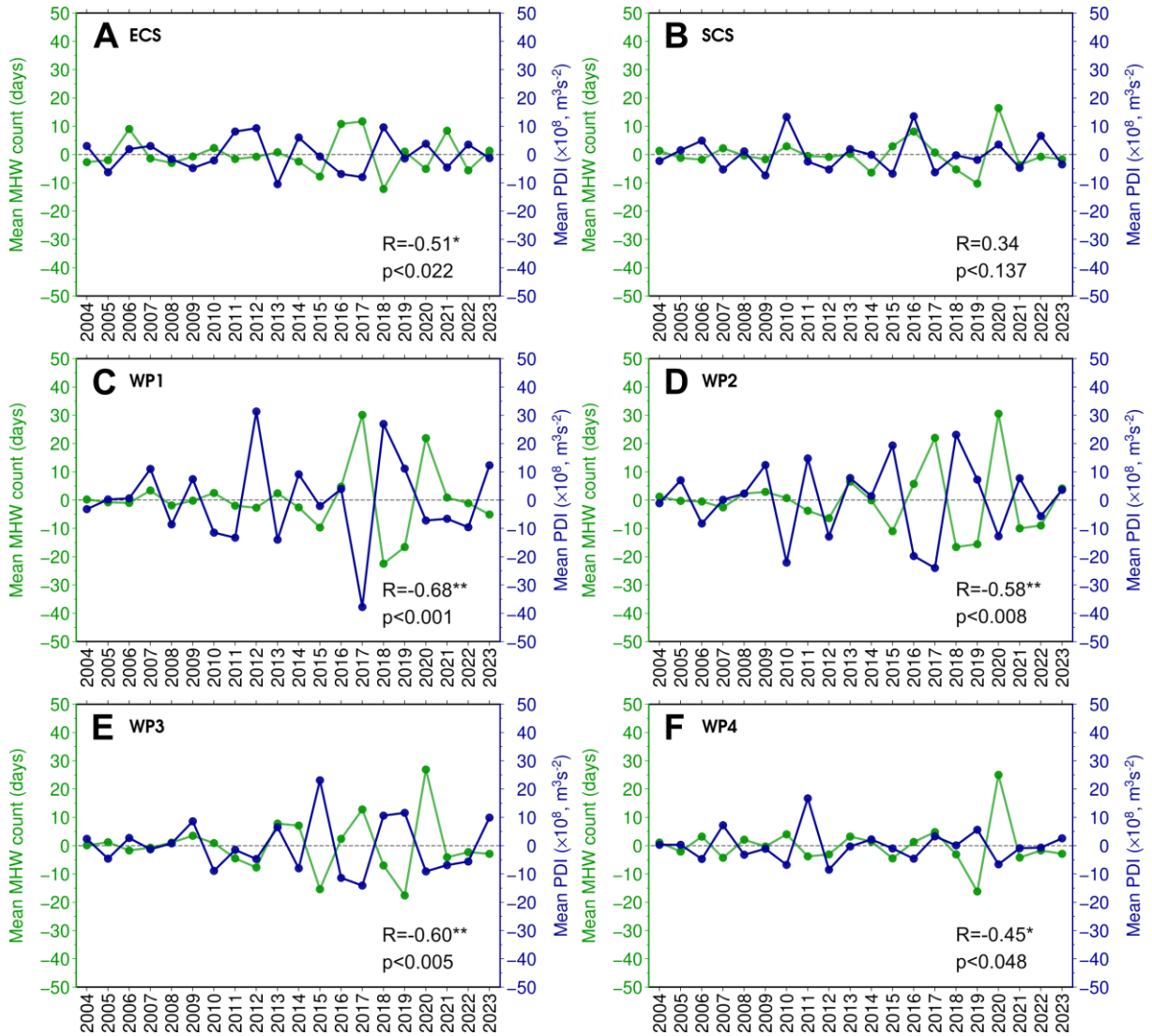


**Fig. S9. Correlation between seasonal MHW days and PDI variations based on NOAA's OISST using a 30-year climatological baseline. (A) ECS. (B) SCS. (C) WP1. (D) WP2. (E) WP3. (F) WP4.** The geographic locations of these sub-regions are shown in Fig. 7. Correlation coefficients and p-values are displayed in the lower-right corners. Note that both time series were detrended with respect to every five-year period, i.e., 2004-2008, 2009-2013, 2014-2018, and 2019-2023. Double asterisks (\*\*) indicate statistical significance at the >99% level, and single asterisk (\*) indicates >90% significance. The baseline period is from 1994 to 2023. The statistical significance was based on Student's t-test.

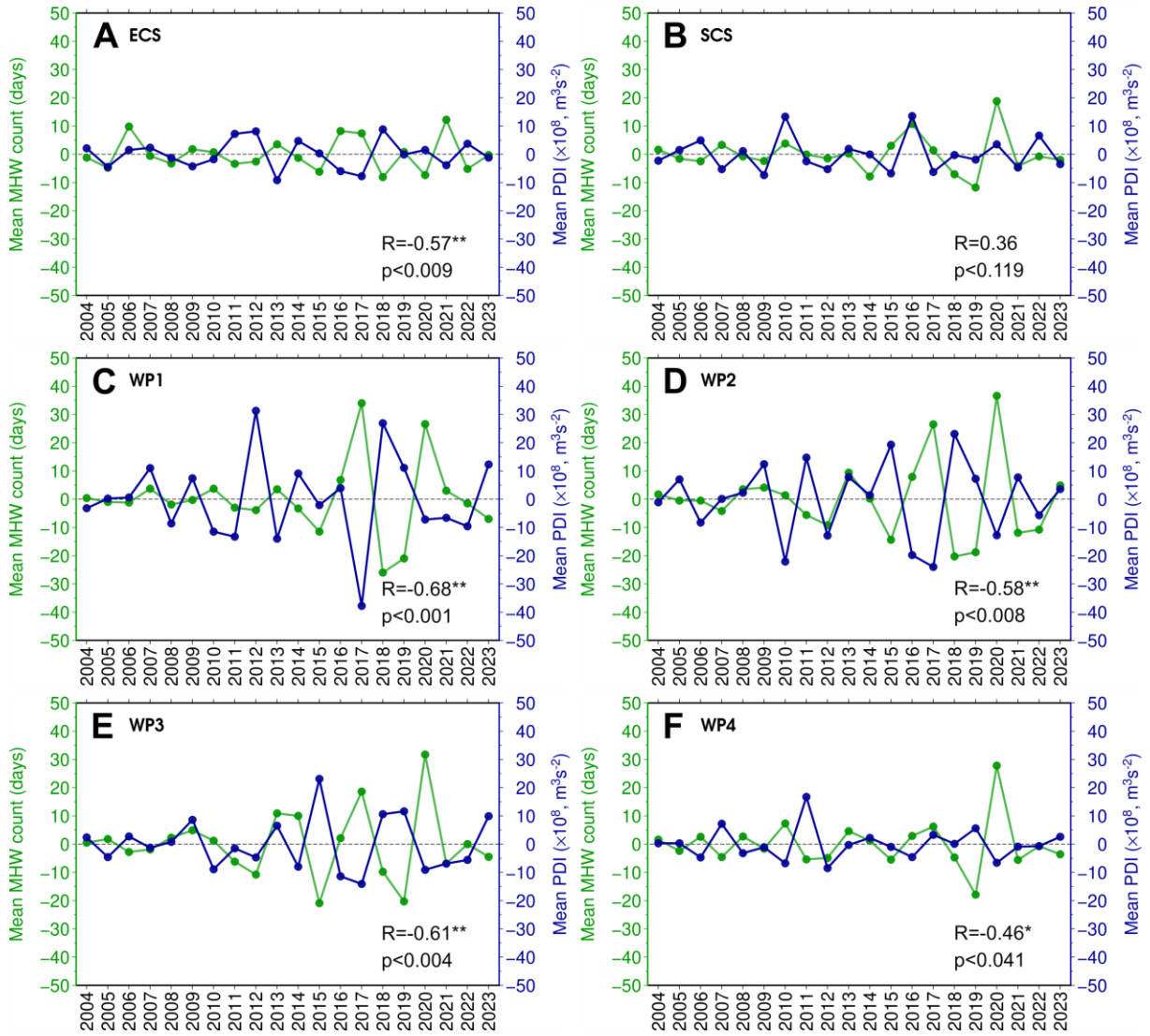


**Fig. S10. Correlation between seasonal MHW days and PDI variations based on NOAA's OISST using a 40-year climatological baseline. (A) ECS. (B) SCS. (C) WP1. (D) WP2. (E) WP3. (F) WP4.** The geographic locations of these sub-regions are shown in Fig. 7. Correlation coefficients and p-values are displayed in the lower-right corners. Note that both time series were detrended with respect to every five-year period, i.e., 2004-2008, 2009-2013, 2014-2018, and 2019-2023. Double asterisks (\*\*) indicate statistical significance at the >99% level, and single asterisk (\*) indicates >90% significance. The baseline period is from 1984 to 2023. The statistical significance was based on Student's t-test.

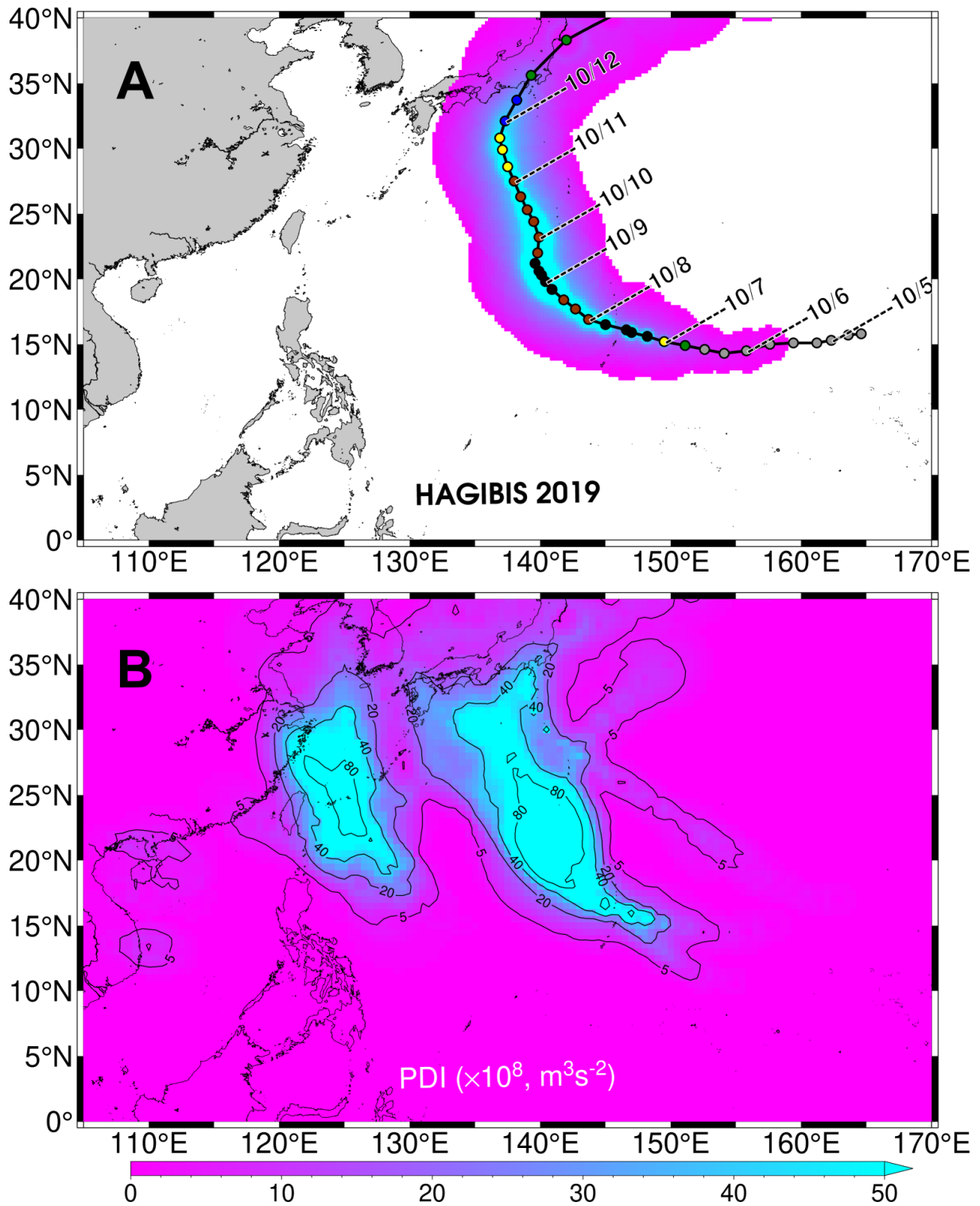


**Fig. S11. Power Dissipation Index (PDI) maps. (A)** PDI calculated from a single Tropical Cyclone Hagibis (2019). **(B)** Seasonally cumulated PDI for 2019.

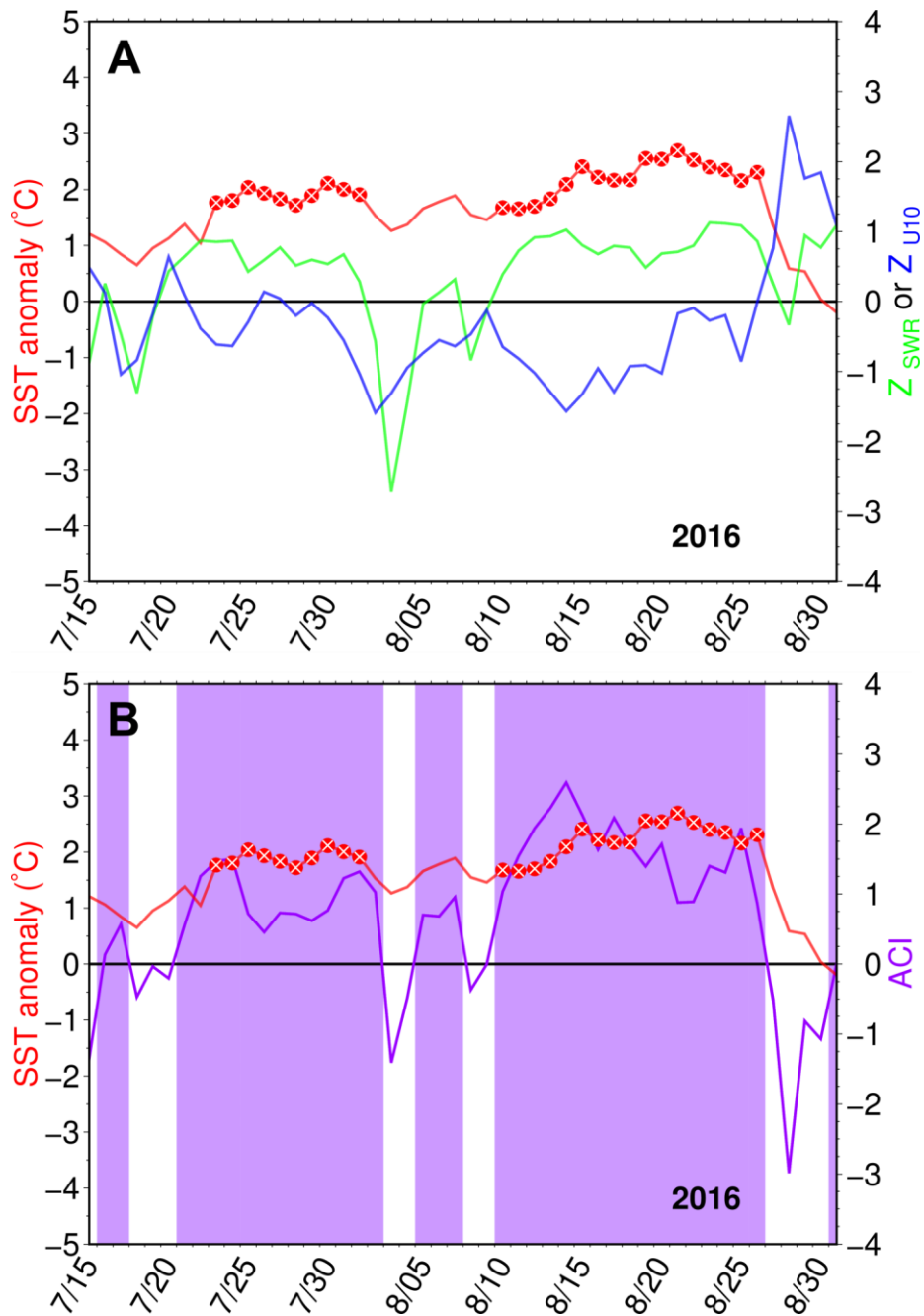


**Fig. S12. SST anomalies and Atmospheric Condition Index (ACI) during the summer of 2016 in the ECS. (A)** SST anomalies versus standardized anomalies of shortwave radiation ( $Z_{SWR}$ ) and 10m wind speed ( $Z_{U10}$ ). **(B)** SST anomalies versus ACI. The SST time series was averaged over the black box region outlined in fig. S1, while the  $Z_{SWR}$ ,  $Z_{U10}$ , and ACI were averaged over the region outlined in figs. S3 and S4. Solid red circles with crosses mark the days identified as MHWs. Purple shading in **(B)** indicates periods with positive ACI values, representing favorable atmospheric conditions for MHW development.

**Table S1. Characteristics of MHWs and TCs for the eight TC-MHW cases identified in the ECS during 2014-2023.** Means and standard deviations ( $\sigma$ ) are shown for each parameter. Asterisks (\*) denote cases in which no MHW occurred through the end of the year following the TC.

<b>TC-MHW cases (yyyyID_name)</b>	<b>Date (yyyymmdd)</b>	<b>Pre-TC MHW duration (days)</b>	<b>SST cooling (°C)</b>	<b>Post-TC MHW count (days)</b>	<b>MHW break (days)</b>	<b>TC intensity (knots)</b>
201720_Talim	20170916	6	1.76	0	*	55
201720_Talim(4)	20170915	5	5.78	11	26	81.3
201812_Ampil	20180722	7	1.98	0	*	55
201818_Yagi	20180812	6	1.62	0	*	45
202009_Bavi	20200825	6	4.44	0	*	97.5
202119_Chanthu(2)	20210913	14	3.60	14	23	85
202119_Chanthu(3)	20210914	15	2.60	21	17	55
202212_Hinamnor	20220905	13	3.14	0	*	105
<b>Mean (<math>\sigma</math>)</b>		<b>9.0 (4.2)</b>	<b>3.1 (1.4)</b>	<b>5.8 (8.4)</b>	<b>22.0 (4.6)</b>	<b>72.3 (22.6)</b>

**Table S2. Characteristics of MHWs and TCs for the 23 TC-MHW cases identified in the SCS during 2014-2023.** Means and standard deviations ( $\sigma$ ) are shown for each parameter. Asterisks (\*) denote cases in which no MHW occurred through the end of the year following the TC.

<b>TC-MHW cases (yyyyID_name)</b>	<b>Date (yyyymmdd)</b>	<b>Pre-TC MHW duration (days)</b>	<b>SST cooling (°C)</b>	<b>Post-TC MHW count (days)</b>	<b>MHW break (days)</b>	<b>TC intensity (knots)</b>
201409_Rammasun	20140718	14	2.75	0	*	131.7
201510_Linfa	20150707	9	3.16	7	130	54.2
201522_Mujigae	20151003	7	1.54	33	41	98.3
201605_Mirinae	20160726	6	0.47	6	116	30
201606_Nida	20160801	5	1.83	7	83	70
201611_Dianmu	20160818	8	1.33	7	70	25
201622_Aere	20161011	8	1.06	5	14	20
201715_Hato	20170822	16	1.58	26	34	85
201721_Doksuri	20170915	10	2.98	0	*	92.5
201724_Khanun	20171015	5	1.01	11	3	90
201905_Invest	20190703	12	1.62	13	15	28.3
202004_Sinlaku	20200730	24	1.38	34	34	15
202013_Noul	20200917	17	1.08	5	3	40
202013_Noul (2)	20200917	23	0.79	15	0	45
202110_Cempaka	20210719	7	1.38	35	56	51.9
202122_Lionrock	20211010	11	1.54	0	*	31.9
202122_Lionrock(2)	20211005	8	1.06	6	45	20
202218_Noru	20220926	14	1.31	0	*	90

202304_Talim	20230717	10	2.35	48	36	70
202309_Saola(2)	20230901	8	2.60	13	62	108
202313_Thirteen	20230925	5	0.97	37	10	25
202314_Koinu	20231007	7	1.81	22	18	99
202316_Sanba	20231018	10	0.84	34	12	33.3
<b>Mean (<math>\sigma</math>)</b>		<b>10.6 (5.3)</b>	<b>1.6 (0.7)</b>	<b>15.8 (14.5)</b>	<b>41.2 (37.5)</b>	<b>58.9 (34.3)</b>

**Table S3. Characteristics of MHWs and TCs for the 54 TC-MHW cases identified in the WP during 2014-2023.** Means and standard deviations ( $\sigma$ ) are shown for each parameter. Asterisks (\*) denote cases in which no MHW occurred through the end of the year following the TC.

<b>TC-MHW cases (yyyyID_name)</b>	<b>Date (yyyymmdd)</b>	<b>Pre-TC MHW duration (days)</b>	<b>SST cooling (°C)</b>	<b>Post-TC MHW count (days)</b>	<b>MHW break (days)</b>	<b>TC intensity (knots)</b>
201408_Neoguri	20140707	7	5.26	16	55	115
201408_Neoguri(2)	20140704	19	1.49	0	*	50
201408_Neoguri(3)	20140705	20	2.09	0	*	90
201408_Neoguri(4)	20140706	19	4.54	0	*	122.5
201410_Matmo	20140723	8	1.43	22	15	70
201413_Fengshen	20140906	7	0.96	0	*	22.5
201416_Fung-wong	20140921	17	1.60	0	*	50
201417_Kammuri	20140925	21	1.55	0	*	40
201503_Kilo	20150907	28	3.70	0	*	72.5
201503_Kilo(2)	20150904	31	3.53	0	*	71.7
201503_Kilo(3)	20150906	11	3.66	0	*	90
201513_Soudelor	20150802	6	1.17	0	*	75
201515_Molave	20150811	9	2.39	0	*	40
201524_Koppu	20151016	5	2.47	0	*	86.7
201602_Nepartak	20160707	14	1.96	12	20	145
201607_Omais	20160805	12	1.24	0	*	47.5
201609_Chanthu	20160813	24	0.50	11	70	30
201612_Lionrock	20160825	15	2.92	25	56	97.5

201616_Meranti	20160912	5	0.61	0	*	155
201705_Nanmadol	20170702	5	0.90	55	10	35
201707_Noru	20170730	11	1.30	54	14	125
201707_Noru(2)	20170723	21	2.68	12	28	80
201711_Nesat	20170728	21	1.81	45	16	67.5
201714_Banyan	20170812	27	0.794	46	36	88
201720_Talim(2)	20170912	11	1.855	26	11	70
201720_Talim(3)	20170913	10	3.078	15	22	90
201725_Lan	20171021	14	2.189	0	*	130
201814_Wukong	20180725	19	1.46	17	21	60
201815_Jongdari	20180728	27	2.595	6	73	85
201817_Shanshan	20180807	6	1.323	17	60	80
201831_Yutu	20181023	10	1.235	0	*	82.5
201909_Francisco	20190802	11	0.674	0	*	40
201911_Krosa	20190806	5	0.432	0	*	40
201914_Faxai	20190907	5	1.803	0	*	115
201914_Faxai(2)	20190908	6	0.843	0	*	115
201920_Hagibis	20191006	8	0.893	0	*	78.3
202006_Six	20200809	7	0.474	85	3	35
202011_Haishen	20200903	17	2.812	21	73	107.5
202011_Haishen(2)	20200902	18	2.014	32	22	65
202012_Twelve	20200911	38	0.538	7	4	20
202014_Dolphin	20200922	9	1.293	0	*	50
202015_Kujira	20200928	29	1.138	33	15	45

202016_Chon-hom	20201005	62	1.733	0	*	30
202119_Chanthu	20210911	8	1.812	0	*	107.5
202120_Mindulle	20210929	15	4.02	0	*	110
202120_Mindulle(2)	20210925	7	2.233	0	*	102.5
202120_Mindulle(3)	20210927	9	5.039	0	*	98.6
202209_Nine	20220811	6	0.712	0	*	27
202211_Tokage	20220823	27	1.377	0	*	72.5
202212_Hinnamnor(2)	20220829	15	1.11	0	*	75
202212_Hinnamnor(3)	20220901	8	4.162	7	32	140
202216_Nanmadol	20220916	7	3.583	5	83	135
202309_Saola	20230826	9	2.148	0	*	104
202315_Bolaven	20231011	9	1.282	6	75	160
<b>Mean (<math>\sigma</math>)</b>		<b>14.7 (10.4)</b>	<b>2.0 (1.2)</b>	<b>10.6 (18.0)</b>	<b>35.4 (26.2)</b>	<b>80.3 (36.0)</b>